ORIGINAL PAPER

Solution versus solid-state electropolymerization of regioregular conjugated fluorenone–thienylene vinylene macromonomers—voltammetric and spectroelectrochemical investigations

**Renaud Demadrille · Malgorzata Zagorska ·
Martial Billon · Guy Louarn · Serge Lefrant ·
Adam Pron**

Abstract We present detailed voltammetric and spectro-electrochemical studies of ***poly(2,7-bis(5-[(E)-1,2-bis(3-octylthien-2-yl)ethylene])-fluoren-9-one)*(PTVF)**—a conjugated polymer consisting of thienylene, vinylene, and fluorenone subunits. PTVF can be easily obtained either by electropolymerization of its monomer (***(2,7-bis(5-[(E)-1,2-bis(3-octylthien-2-yl)ethylene])-fluoren-9-one)*** [TVF]) dissolved in the electrolytic solution or via solid-state electropolymerization of a thin film of the monomer deposited on the electrode. UV-vis-NIR spectroscopic data indicate that the latter method leads to a polymer of a smaller degree of polymerization (DP). The possibility of the formation of a polymeric conductor on a transparent conductive substrate such as indium tin oxide, in situ, via solid-state electropolymerization, combined with its post-polymerization transformation into an organic semiconductor by electrochemical dedoping, is technologically very attractive and makes TVF and its polymer very promising materials for applications in organic electronics.

Keywords Fluorenone · Solid-state polymerization · UV-vis-NIR and Raman Spectroelectrochemistry

R. Demadrille · M. Billon · A. Pron (✉)
DRFMC, UMR 5819-SPrAM (CEA-CNRS-Univ. J. Fourier-Grenoble I), Laboratoire d'Electronique Moléculaire Organique et Hybride, CEA Grenoble,
17 Rue des Martyrs,
38054 Grenoble Cedex 9, France
e-mail: adam.pron@cea.fr

M. Zagorska
Faculty of Chemistry, Warsaw University of Technology,
00 664 Warszawa Noakowskiego 3,
Warsaw, Poland

G. Louarn · S. Lefrant
Institut des Matériaux Jean Rouxel (IMN),
B. P. 32229,
44322 Nantes Cedex 3, France

Introduction

Synthesis of specially designed conjugated macromonomers, which can then be polymerized to give the corresponding electroactive polymers, has become, in the past decade, one of the most exploited routes for the preparation of new materials of interest in organic electronics and electrochemistry [1]. There are several advantages of this approach. First, by imposing an appropriate symmetry of the macromonomer, it is possible to obtain polymers of the desired regioregularity [2–4]. Second, the electronic and electrochemical properties of the polymer being designed can conveniently be tuned by introduction of electron-donating (withdrawing) groups as inherent parts of the macromonomer, which then modify the π-electron density in the resulting polymer [5–7].

Macromonomers are usually transformed into polymers using oxidative (chemical or electrochemical) polymerization [8–11] or, after appropriate functionalization of their end groups, via polycondensation [12]. Several instructive examples of this approach can be given, among them, for example, recent preparation of a polythiophene derivative with enhanced charge carriers' mobility with the aim to use it in the fabrication of organic field effect transistors [13].

In the search for new materials suitable for the fabrication of organic photovoltaic cells, we have synthesized a new macromonomer consisting of fluorenone and thienylene vinylene subunits—*(2,7-bis(5-[(E)-1,2-bis(3-octylthien-2-yl)ethylene])-fluoren-9-one)* (see Fig. 1), abbreviated in the subsequent text as *TVF* [14]. In addition to its promising electronic properties, TVF exhibits interesting electrochemistry as it may undergo both solution and solid-state polymerization. The latter phenomenon is rare in polymer chemistry, in general, and in electrochemical polymerization of conjugated polymers, in particular [15, 16]. The solid-state electropolymerization is, however, of technological interest, especially in organic electronic technology, as it allows for a facile formation of polymers in macromonomer layers predeposited on suitable electrodes. In this paper, we present, for the first time, a comparative study of the solution and solid-state electropolymerization process of TVF using cyclic voltammetry supported by UV-vis and Raman spectroelectrochemistry.

Experimental

Electrochemical polymerization of TVF and cyclic voltammetry

The synthetic pathway leading to the macromonomer (TVF) as well as the detailed preparation procedure can be found in [14].

Two types of electrochemical polymerizations have been carried out: solution and solid-state electropolymerizations.

Solution electropolymerization was carried out in the electrolyte consisting of 0.1 M Bu_4NBF_4 in methylene chloride in which an appropriate amount of TVF was dissolved as to give 0.1 M solution with respect to the monomer. The electropolymerization was carried out in a one compartment electrolytic cell with a working platinum electrode of 0.07 cm^2 surface area, a platinum counter-electrode, and an Ag/0.01 Ag^+ reference electrode. The potential of the reference electrode measured vs. ferrocene couple in the same electrolytic solution was 0.08 V. The polymer was deposited on the working electrode by consecutive potential scans in the potential range from -0.20 to +0.60 V, with the scan rate of 20 mV/s.

In a set of separate experiments designed for spectro-electrochemical investigations, the polymer was deposited on an indium tin oxide (ITO) electrode (for UV-vis-NIR

spectroscopy) or on a platinum electrode (for Raman spectroscopy) using the same electrolytic solution containing TVF, as described above.

Before cyclic voltammetry and spectroelectrochemical investigations, the polymer deposited on the electrode was repeatedly washed with methylene chloride and then with acetonitrile with the goal to remove small amounts of excess TVF adsorbed on the surface of the films. The cyclic voltammetry measurements of the electropolymerized films were carried out in 0.1 M Bu_4NBF_4 acetonitrile using the same electrolytic cell and the same set of electrodes, which were used for the electropolymerizations. The same electrolytic solution was used for spectroelectrochemical investigations of electropolymerized films. The UV-vis-NIR spectra of the polymer film were recorded on a Lambda 2 Perkin Elmer spectrometer, whereas the Raman spectra were obtained using a FT Raman Bruker RFS 100 spectrometer with the near-IR excitation line (1,064 nm).

Solid-state electropolymerization was performed in the same electrolytic cell, which was used for the solution polymerization and with the same set of electrodes. A thin layer of TVF was first deposited on the surface of the working electrode and carefully washed with acetonitrile. The electropolymerization was then carried out in the monomer-free electrolyte consisting of 0.1 M Bu_4NBF_4 in acetonitrile by repeated cycling the potential between −0.30 and +0.50 V with the scan rate of 20 mV/s. In these conditions, the layer initially deposited on the working electrode remained insoluble throughout the whole electropolymerization process.

In two sets of separate experiments, the solid-state electropolymerization was followed by UV-vis-NIR and Raman spectroelectrochemistry using the IR excitation line (λ_{exc}=1,064 nm). In the former case, a thin TVF layer was deposited on an ITO electrode, whereas in the latter on a platinum electrode with the composition of the electrolytic solution remaining the same as described above.

Results and discussion

In Fig. 2a, the first seven scans of the solution voltammetric electropolymerization of TVF are presented. The observed features are typical of electropolymerizable conjugated monomers, i.e., the irreversible peak at higher potentials corresponds to the polymerization process initiated by coupling of radical cations. The broad redox couple at

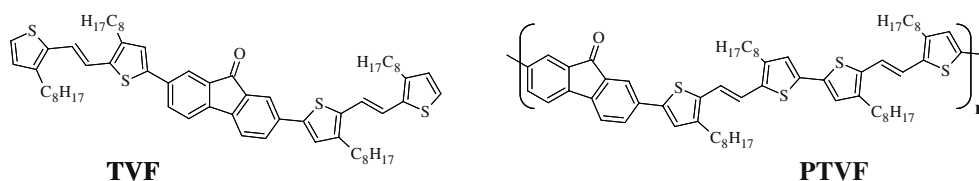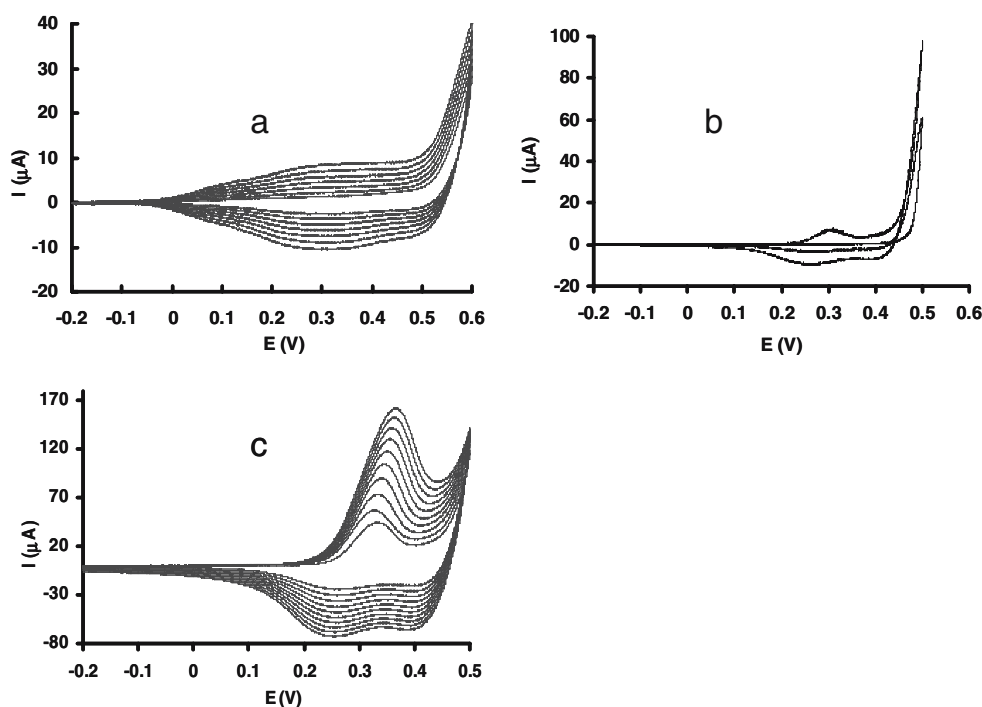**Fig. 1** Chemical formulae of TVF and PTVF

TVF   **PTVF**

Fig. 2 Voltammetric polymerizations of TVF. **a** Solution polymerization in 0.1 M Bu$_4$NBF$_4$ in CH$_2$Cl$_2$ containing 0.1 M of TVF. **b** First two scans of solid-state polymerization in 0.1 M Bu$_4$NBF$_4$ in acetonitrile. **c** Consecutive scans of solid-state polymerization in 0.1 M Bu$_4$NBF$_4$ in acetonitrile. Scan rate 20 mV/s, E vs. Ag/0.01 Ag$^+$

lower potentials is associated with the oxidative doping and reductive dedoping of the polymer deposited on the electrode. A steady increase of the area of the doping/dedoping peaks with increasing scan number indicates that the polymerization process occurs smoothly and is not perturbed by the increasing thickness of the growing polymer film.

The first two scans of the anodic solid-state polymerization of TVF are shown in Fig. 2b. In the first scan, the deposited solid monomer layer remains electrochemically inactive for a very large potential range and starts to oxidize at potentials very close to that of the vertex potential (E=+0.50 V). As a result of this anodic oxidation, an electroactive polymer is formed in the doped (cationic) form, whose presence is manifested twice: (1) in the reverse scan of the first cycle by a clear cathodic peak associated with its reductive dedoping, i.e., the transformation of the polycationic form into the neutral one and (2) in the anodic part of the second scan as a peak originating from the doping of the neutral form, i.e., from the transformation of the neutral chains into polycations. Thus, polarization of the electrode to E = +0.50 V results in the appearance of a new redox couple in the potential range where the deposited solid monomer (TVF) is electrochemically inactive.

Solid-state polymerization of phenylene and thienylene "homo-oligomers" has been studied in detail by Meerholz and Heinze [15] who have shown that their oxidation to dications is reversible and does not result in any consecutive polymerization reaction. The polymerization starts as soon as trications appear. This is evidently not the case for the

"ter-oligomer" studied in this research, which contains three electrochemically active groups of different chemical nature. For TVF, the onset of the oxidation involves irreversible follow-up polymerization reactions. Upon consecutive scanning of the potential between −0.30 and +0.50 V, a steady increase of the intensity of the polymer doping/dedoping redox couple is observed (Fig. 2c), similarly as in the case of the solution electropolymerization, proving that during each scan a new fraction of the monomer present on the electrode is transformed into the polymer.

It should be noticed that the potential ranges of the electrochemical doping of the polymer and the electro-polymerization of the monomer are well separated. It is therefore possible to investigate the electrochemical doping of the polymer formed without any interference from the monomer also present at the electrode. Figure 3a and c compare cyclic voltammograms of products obtained by the solution and solid-state polymerizations, respectively.

The presence of easily oxidizable vinylene groups in the conjugated backbone of PTFV significantly lowers the potential of the oxidative doping as compared to its analogue consisting of thienylene and fluorenone subunits [17, 18]. The cyclic voltammogram of the polymer prepared via solution polymerization is typical of electro-active polymers of the polythiophene family and consists of one broad doping peak with a maximum at +0.23 V followed by a plateau of the capacitive current originating from the introduction of dopant anions to the polymer matrix, compensating the charge of polycations created upon the doping process. The oxidative doping peak has its
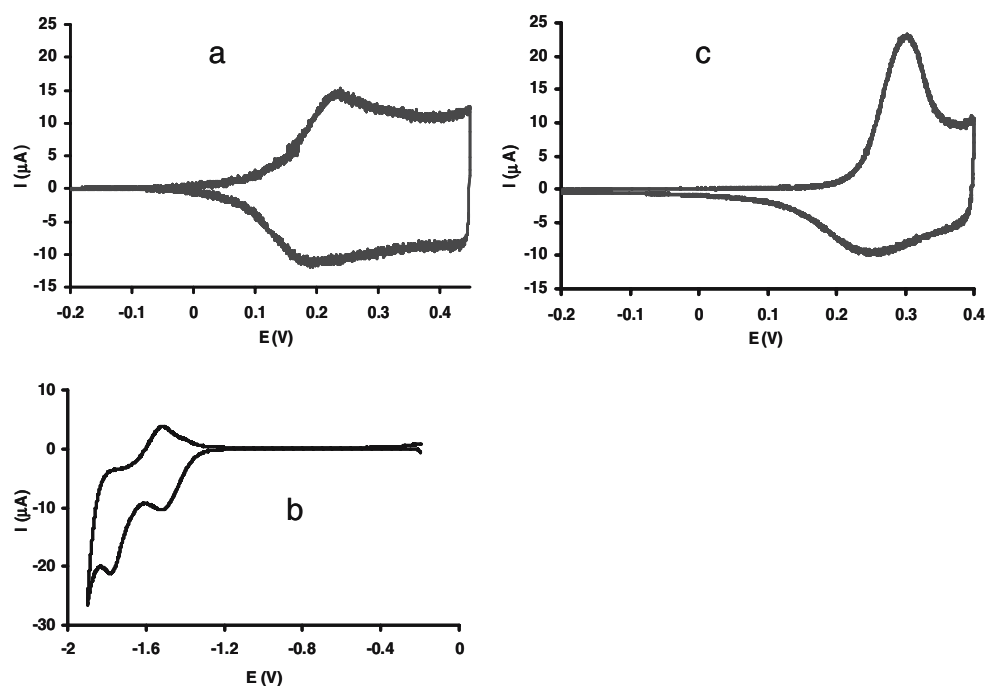
cathodic counterpart peaked at $E = +0.18$ V, ascribed to the reductive dedoping.

The cyclic voltammogram of the oxidation PTVF prepared by the solid-state polymerization method, is somehow different. We observe a much narrower peak of the oxidative doping that, in addition, is shifted towards higher potentials by approximately 75 mV as compared to the corresponding peak in PTVF deposited by solution electropolymerization. It is known that in the polythiophene family of conjugated polymers, the position of this peak is strongly molecular-weight-dependent, with increasing degree of polymerization (DP) being increasingly displaced to lower potentials [19]. Thus, the registered cyclic voltammograms unequivocally indicate that fractions of lower molecular weight are obtained by the solid-state polymerization procedure, and the resulting product is more resistant towards oxidative doping.

The chemical constitution of PTVF also implies its reducibility associated with the presence of fluorenone subunits and with the reductive (*n*-type) doping of the polymer backbone. Figure 3b shows a representative cyclic voltammogram covering the potential range of the PTVF reduction. Its shape indicates that the reduction of the polymer is a double step process. We assign the first peak, with a minimum at $E = -1.52$ V, to the reduction of the carbonyl group of the fluorenone moiety as, its position is very close to that of the corresponding peak in poly(fluorenone) homopolymer if the correction for the reference electrode potential is taken into account [20]. We are tempted to attribute the second reduction peak to the *n*-doping of the polymer. Similar double-step reduction, although shifted to lower potentials, has recently been

found for an alternate copolymer of fluorenone—dialkylbithiophene with no vinylene subunits [21].

Containing three spectrally complementary chromophores, which, in addition, are in conjugation, the neutral form of chemically prepared PTVF shows an absorption spectrum covering almost the entire range of the visible spectrum [14]. This applies also to the solution electropolymerized PTVF (Fig. 4). At $E = -0.36$ V, the spectrum consists of one broad absorption band with a clear vibrational structure. Consistent with the cyclic voltammogram (compare Figs. 3a and 4), the doping-induced spectral changes start at $E = +0.09$ V and are manifested by a decrease in the intensity of the band originating from the neutral conjugated polymer backbone with a simultaneous growth of a broad band in the near infrared part of the spectrum, characteristic of the doped state [22]. Note that a
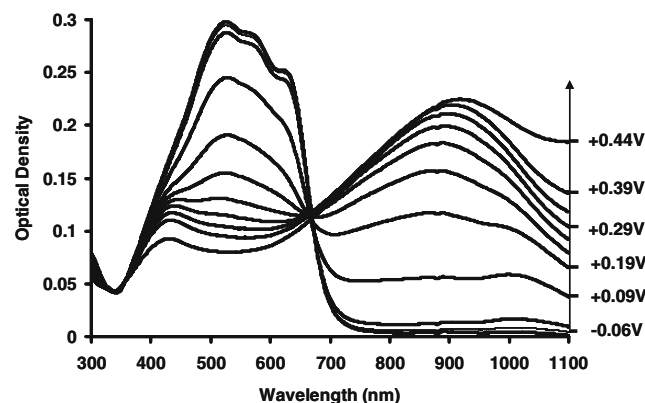
Fig. 4 UV-vis-NIR spectra of a thin film of solution-polymerized PTVF registered for increasing electrode potentials. Electrolyte, 0.1 M Bu_4NBF_4 in acetonitrile; E vs. Ag/0.01 Ag^+

small band at 430 nm, which in the spectrum of the neutral polymer is present only as a shoulder of the broad dominant band, does not bleach upon electrochemical doping and becomes clearly visible in the spectra registered at higher potentials. Following [23], we attribute this band to the $n-\pi^*$ transition of the carbonyl group in the fluorenone subunit. This result seems to indicate that the carbonyl group does not participate in the charge redistribution associated with the doping process.

UV-vis-NIR spectroscopy seems especially suitable for in situ investigations of the solid-state polymerization of TVF as the polymerization and doping processes involve profound changes in this spectral range. Fig. 5 shows the spectrum of a thin film the monomer registered at the open-circuit conditions ($E_{oc} = -0.36$ V). The spectrum is dominated by a relatively narrow band at 400 nm accompanied with a distinct shoulder at higher wavelengths. Polarization of the electrode to the potentials corresponding to the onset of the solid-state electropolymerization process ($E=+0.50$ V) results in a dramatic evolution of the UV-vis-NIR spectrum (see Fig. 5). We can notice two principal changes: (1) the band at approximately 425 nm decreased significantly, although it did not disappear completely and (2) a new broad band appeared in the NIR part of the spectrum, similar to that observed for doped PTVF obtained via solution electropolymerization (compare Figs. 4 and 5). The presence of this band can be taken as the first indication of the electropolymerization process.

The most significant difference between the spectra of doped PTVF, obtained in the solution and solid-state polymerizations, is a higher relative intensity of the band at 425 nm in the latter. This is not unexpected as, in addition to the $n-\pi$ band of the carbonyl group, it contains
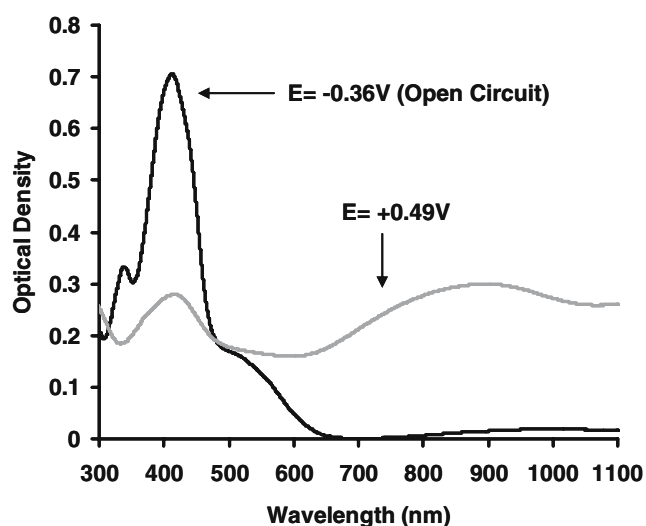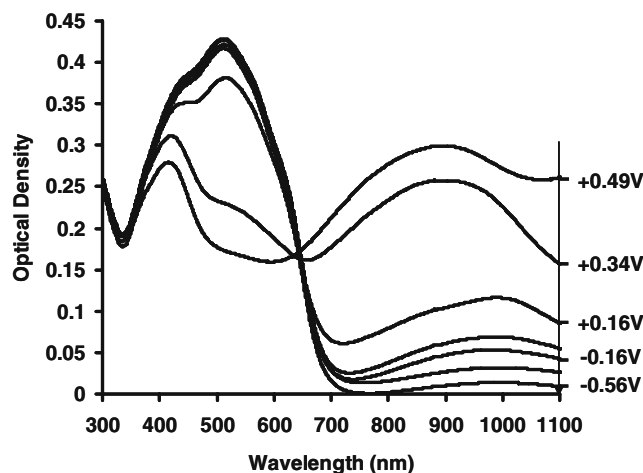

Fig. 6 UV-vis-NIR spectra of solid-state polymerized PTVF registered in the reduction mode, i.e., for decreasing electrode potentials. Electrolyte, 0.1 M Bu$_4$NBF$_4$ in acetonitrile; E vs. Ag/0.01 Ag$^+$

the contribution from the band originating from nonpolymerized TVF, as the two coincide.

In this perspective, electrochemical reduction of the polymerization product to its neutral state should provide experimentum crucis for the solid polymerization process. Figure 6 shows the evolution of its UV-vis-NIR spectra with a decreasing electrode potential.

Reductive removal of the dopant results in a decrease of the band in the NIR part of the spectrum, attributed to the doped state, which for $E=-0.56$ V disappears completely. In the same time, the band characteristic of the neutral state grows in intensity. The presence of an isosbestic point indicates that the dedoping process is not accompanied by other side reactions.

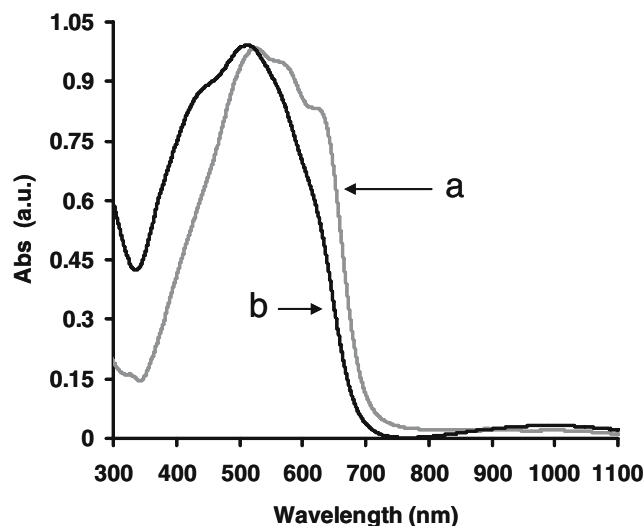In Fig. 7, the spectra of the neutral forms of PTVF obtained by the solution and solid-state polymerizations are

Fig. 5 UV-vis-spectra of a thin film of TVF registered at the open circuit potential ($E_{oc} = -0.36$ V) and at $E = +0.49$ V. Electrolyte, 0.1 M Bu$_4$NBF$_4$ in acetonitrile; E vs. Ag/0.01 Ag$^+$

Fig. 7 Comparison of the UV-vis-NIR spectra of the neutral form of PTVF obtained: **a** by solution electropolymerization and **b** by solid-state polymerization

compared. The dominant absorption band of the latter is hypsochromically shifted as compared to the case of the former. This can be taken as another indication of a lower DP for the polymer obtained by the solid-state synthesis. Some differences in the higher energetic part of the spectra of both polymers should also be noted, associated with the presence of nonpolymerized monomer, in the case of the solid-state polymerization, which give rise to a band in the vicinity of 425 nm.

To summarize, a profound spectral change of the irreversible nature involving a significant bathochromic shift of the absorption bands, observed after the oxidation–reduction sequence, can be taken as a clear spectroscopic manifestation of the solid-state polymerization process.

Both doping and polymerization processes give rise to significant changes in the bond configurations and in the bond force constants. All these changes can be followed by vibrational spectroscopies. For these reasons, we were tempted to investigate both types of PTVF by Raman spectroscopy. Figure 8 shows the Raman spectroelectrochemical data obtained for the doping of PTVF deposited on the electrode by solution electropolymerization.

The neutral form of the polymer contains bands originating from all three structural subunits. In particular bands at 1,422 and 1,396 cm^{-1}, we ascribe to the stretching deformations C_α–C_β and C_β–C_β in the thienylene subunits [24, 25]. The band at 1,597 cm^{-1} without any ambiguity can be ascribed to the fluorenone subunit. Note that the C=O-stretching band of fluorenone is not observed. Bands at 1,531 and 1,298 cm^{-1} must originate from the stretching and bending deformations of the vinylene subunits as they are absent in alkyl derivatives of polythiophene [24] and in alternate copolymers containing oligothiophene and fluorenone units [18].

Consistent with the cyclic voltammetry and UV-vis-NIR results, first doping-induced spectral changes are observed at $E = +0.04$ V and is manifested by the slight lowering of the intensity of the bands at 1,597 and 1,422 cm^{-1},
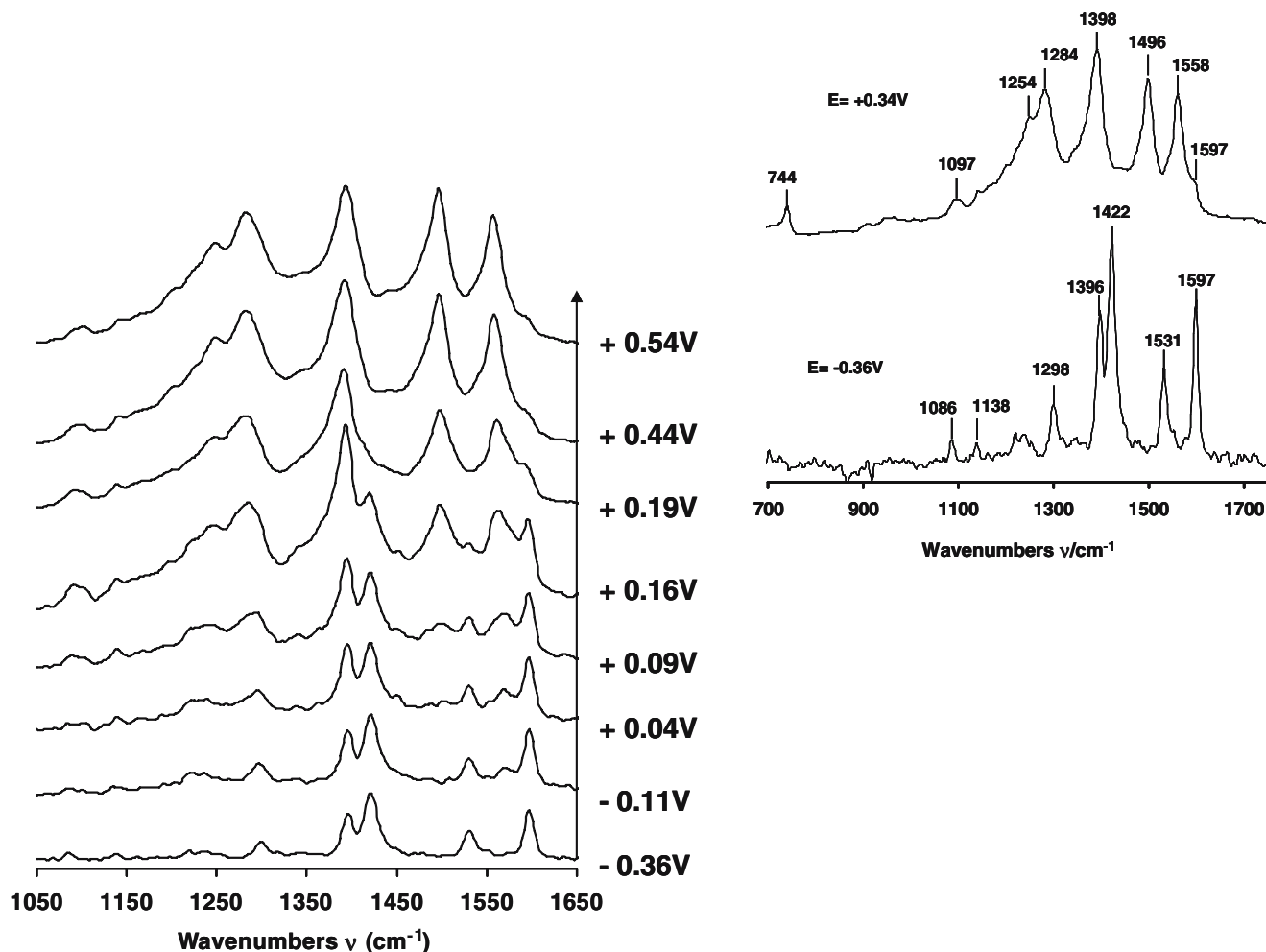

Fig. 8 Raman spectra of a thin film of PTVF registered for increasing electrode potentials. λ_{exc}=1,064 nm; electrolyte, 0.1 M Bu$_4$NBF$_4$ in acetonitrile; E vs. Ag/0.01 Ag$^+$

characteristic of the neutral state with simultaneous appearance of new bands in the vicinity of 1,560, 1,500, and 1,250 cm^{-1}, characteristic of the doped state. These changes are amplified for higher electrode potentials. Bands originating from the undoped polymer coexist with those characteristic of its doped form up to $E = +0.16$ V. Above this potential value, the spectrum becomes typical of the doped polymer and undergoes no further evolution. Thus, Raman spectroscopy does not detect the presence of undoped parts of the polymer despite the fact that, at this potential, the doping is far from saturation. Such behavior is connected with a strong resonance enhancement of the Raman scattering originating from the doped form of the polymer, observed for the infrared excitation line ($\lambda_{exc}=$ 1,064 nm) [26, 27]. Doping-induced bathochromic shift of Raman bands together with the appearance of the C_α–$C_{\alpha'}$ thiophene interring-stretching bands at 1,254 cm^{-1} is consistent with the overall bond order lowering associated with the transformation of the neutral polymer chains into polycations as well as with the change of the bond sequence from aromatic to quinoïd [28–30].

We have used FT Raman spectroelectrochemistry to follow the TVF solid-state electropolymerization with the goal to verify whether the conclusions derived from UV-vis-NIR studies are also confirmed by Raman spectroscopy. In Fig. 9, the spectrum TVF registered at the open-circuit potential ($E_{oc} = -0.36$ V) is compared with that registered after the electrode polarization to $E = +0.49$ V.

We notice a relatively high signal to noise ratio in the spectrum of neutral TVF. This is not unexpected as the macromonomer shows a negligible absorbance at 1,064 nm (see Fig. 5), and the spectrum is registered in out-of-resonance conditions. For these reasons, only the most intensive peaks are visible at 1,416, 1,451, and 1,601 cm^{-1}. The two former peaks are attributed to the 2,5-thienylene
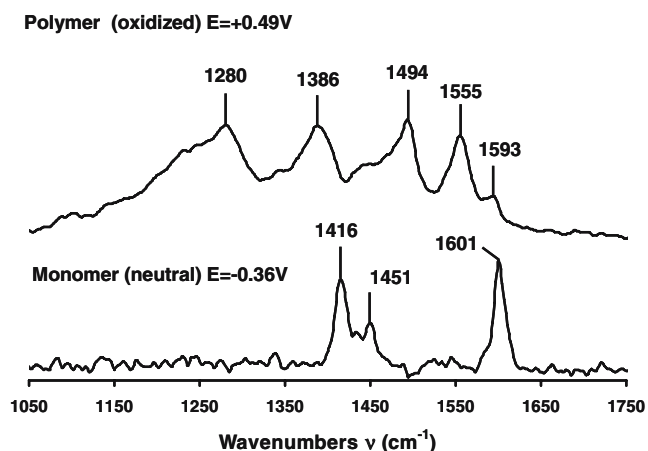
subunits, whereas the latter to the fluorenone ones. The band originating from the vinylene groups stretching is hardly visible in the vicinity of 1,525 cm^{-1}.

Polarization of the electrode at $E=+0.49$ V results in a significant increase of the absorbance at 1,064 nm (Fig. 5), improving in this manner the resonance conditions for the Raman scattering. The spectrum, recorded at this potential, strikingly resembles that of electrochemically doped PTVF (see Fig. 8, spectrum registered at $E=+0.54$ V). Because of the lack of the resonance, lines originating from non-polymerized TVF (still present at the electrode together with solid state polymerized PTVF) are weak and present as shoulders of the dominant lines.

Similarly, as in the case of UV-vis-NIR studies, the solid-state electropolymerization is clearly manifested by significant changes of the Raman spectra in the stepwise reduction of the film previously polarized to $E=+0.49$ V, which evolve towards those characteristic of neutral PTVF rather than neutral TVF (Fig. 10).

At $E=-0.56$ V, in addition to all bands characteristic of neutral PTVF (1,597, 1,526, 1,420, 1,293 cm^{-1}), we observe one additional band at 1,569 cm^{-1} originating from incomplete reduction of the polymer, which is also manifested in the UV-vis-NIR spectrum by a small but measurable absorbance at 1,064 nm (see Fig. 6). As the infrared excitation line is "oversensitive" towards the doped form of PTVF, even small amounts of the doped phase give rise to relatively intensive Raman bands. Finally, the bands
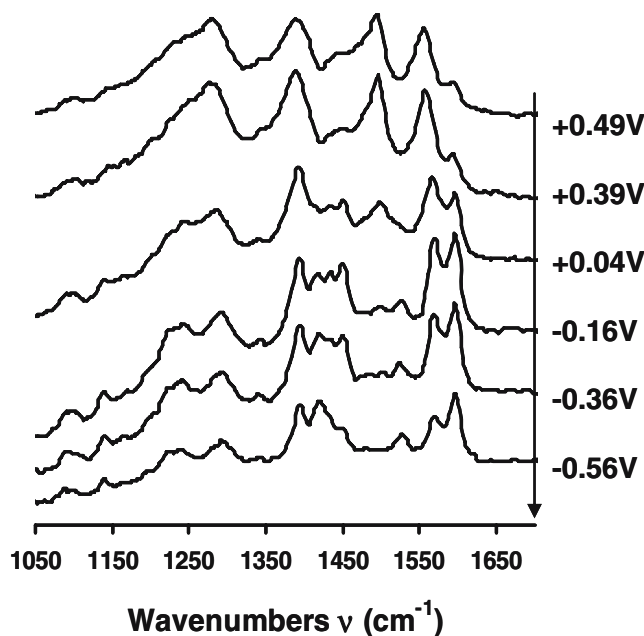

Fig. 9 Raman spectra of a thin film of TVF registered at the open circuit potential ($E_{oc} = -0.36$ V) and at $E = +0.49$ V. $\lambda_{exc}=1,064$ nm; electrolyte, 0.1 M Bu$_4$NBF$_4$ in acetonitrile; E vs. Ag/0.01 Ag$^+$

Fig. 10 Raman spectra of solid-state polymerized PTVF registered in the reduction mode, i.e., for decreasing electrode potentials. $\lambda_{exc}=1,064$ nm; electrolyte, 0.1 M Bu$_4$NBF$_4$ in acetonitrile; E vs. Ag/0.01 Ag$^+$

originating from nonpolymerized TVF can also be detected as shoulders of the existing peaks. Thus, the results of Raman spectroscopy fully support the concept of solid-state electropolymerization of TFV derived from cyclic voltammetry and UV-vis-NIR data.

Conclusions

To conclude, the voltammetric behavior of TVF unequivocally indicates that this macromonomer, if deposited on the electrode in a form of a thin film, can undergo solid-state polymerization. The electrochemical and spectroelectrochemical properties of the solid-state polymerized material are similar to those determined for PTVF obtained via chemical or electrochemical solution polymerization, despite the fact that its DP is lower.

References

1. Fichou D (1999) Handbook of oligo- and polythiophenes. Wiley–VCH, New York
2. Liu B, Yu WL, Lai YH, Huang W (2000) Macromolecules 33:8945–8952
3. Wang WL, Lai YH (2002) Thin Solid Films 417:211–214
4. Demadrille R, Divisia-Blohorn B, Zagorska M, Quillard S, Lefrant S, Pron A (2005) Electrochim Acta 50:1597–1603
5. Xu JM, Ng SC, Chan HSO (2001) Macromolecules 34:4314–4323
6. Levi MD, Fisyuk AS, Demadrille R, Markevich E, Gofer Y, Aurbach D, Pron A (2006) Chem Commun 3299–3301
7. Fisyuk AS, Demadrille R, Querner C, Zagorska M, Bleuse J, Pron A (2005) New J Chem 29(5):707–713
8. Catellani M, Luzzati S, Musco A, Speroni F (1994) Synth Met 62:223–228
9. Demadrille R, Rannou P, Bleuse J, Oddou JL, Pron A, Zagorska M (2003) Macromolecules 36:7045–7054
10. Ong BS, Yiliang W, Liu P, Gardner S (2004) J Am Chem Soc 126:3378–3379
11. Campos LM, Tontcheva A, Günes S, Sonmez G, Neugebauer H, Sariciftci NS (2005) Chem Mater 17:4031–4033
12. Coppo P, Cupertino DC, Yeates SG, Turner ML (2003) Macromolecules 36:2705–2711
13. Mcculloch I, Heeney M, Bailey C, Genevicius K, Macdonald I, Shkunov M, Sparrowe D, Tierney S, Wagner R, Zhang WM, Chabinyc ML, Kline RJ, Mcgehee MD, Toney MF (2006) Nat Mater 5:328–333
14. Demadrille R, Firon M, Leroy J, Rannou P, Pron A (2005) Adv Funct Mater 15:1547–1552
15. Meerholz K, Heinze J (1996) Electrochim Acta 41:1839–1854
16. Fabre B, Marrec P, Simonet J (1998) J Electrochem Soc 145:4110–4119
17. Levi MD, Demadrille R, Pron A, Vorotyntsev MA, Gofer Y, Aurbach D (2005) J Electrochem Soc 152:E61–E67
18. Demadrille R, Divisia-Blohorn B, Zagorska M, Quillard S, Rannou P, Travers JP, Pron A (2003) New J Chem 27:1479–1484
19. Pokrop R, Verilhac JM, Gasior A, Wielgus I, Zagorska M, Travers JP, Pron A (2006) J Mater Chem 16(30):3099–3106
20. Uckert F, Setayesh S, Muller K (1999) Macromolecules 32:4519–4524
21. Levi MD, Demadrille R, Markevich E, Gofer Y, Pron A, Aurbach D, Pron A (2006) Electrochemistry Communications 8:993–998
22. Chung T, Kaufman JH, Heeger AJ, Wudl F (1984) Phys Rev B 30:702–710
23. Jaramillo-Isaza F, Turner ML (2006) J Mater Chem 16:83–89
24. Louarn M, Trznadel M, Buisson JP, Laska J, Pron A, Lapkowski M, Lefrant S (1996) J Phys Chem 100:12532–12539
25. Pron A, Lapkowski M, Zagorska M, Glowczyk-Zubek J, Louarn G, Lefrant S (1996) In: Kajzar F, Agranovich VM, Lee CYC (eds) Photoactive organic materials, science and applications. NATO ASI Ser Partnersh Sub-ser 3 High Technol 9:34
26. Furukawa Y (1996) J Phys Chem 100(39):15644–15653
27. Lefrant S, Buisson JP, Baitoul M, Orion I (1996) Pure Applied Opt 5:613–620
28. Casado J, Hernandez V, Hotta S, Lopez-Navarrete JT (1998) Adv Mater 10:1458–1461
29. Cuff L, Kertesz M (1997) J Chem Phys 106(13):5541–5553
30. Trznadel M, Zagorska M, Lapkowski M, Louarn M, Lefrant S, Pron A (1996) J Chem Soc Faraday Trans 92:1387–1394